

Characterization and modelling of the spatial heterogeneity of snowmelt erosion

G. Ollesch,^{1*} Y. Sukhanovski,² I. Kistner,¹ M. Rode³ and R. Meissner⁴

¹ UFZ Centre for Environmental Research, Department of Soil Science, Brueckstr. 3a, 39114 Magdeburg, Germany

² The All Russian Research Institute of Agronomy and Soil Erosion Control, Karl Marx Str. 70B, Ru-305021 Kursk, Russia

³ UFZ Centre for Environmental Research, Department of Hydrological Modelling, Brueckstr. 3a, 39114 Magdeburg, Germany

⁴ Centre for Environmental Research, Department of Soil Science, Dorfstr. 55, D-39615 Falkenberg, Germany

*Correspondence to: G. Ollesch,
UFZ Centre for Environmental
Research, Department of
Soil Science, Brueckstr. 3a,
39114 Magdeburg, Germany.
E-mail: gregor.ollesch@ufz.de

Abstract

Recent studies about soil erosion show that erosion rates in winter can reach or exceed erosion induced by summer events. A factor of particular importance is the incidence of frozen soil, which modifies the surface runoff generation and also the erodibility of the soil. In this paper, investigations are conducted to characterize the snowmelt erosion events in the 1.44 km² 'Schäfertal' research catchment that is located c. 150 km southwest of Berlin. Two runoff events of different initial conditions are compared and analysed. Although the net erosion rate in the catchment is relatively low, the described event with soil frost is considerably different from the event without soil frost. For example, the net erosion, maximum and median suspended sediment concentrations are significantly higher for the event with frozen soil. The results presented suggest that the sediment source areas differ for both situations. On one hand the channel or sediment flushing is identified as the source, while on the other hand hill slope processes and intra-storm variations are recognized for the soil frost situation. A model modification is presented to improve the estimation of spatial differentiation of surface runoff within the continuous hydrological model WaSim, which is linked to the erosion model AGNPS. Based on measurements of topsoil temperature at locations with diverse exposition and land use, an algorithm is developed. The average agreement of air temperature to the calculated topsoil temperature is $r^2 = 0.75$. The spatial information about soil frost is utilized to modify the infiltration characteristics of the soil. Hence, the spatial aspects of runoff generation in winter conditions and the related transport of sediment is considered in a more realistic way. The spatial results of the modelling are plausible but the estimation of erosion needs further improvement. Copyright © 2005 John Wiley & Sons, Ltd.

Keywords: snowmelt; soil frost; erosion; AGNPS; WaSim

Received 20 January 2003;
Revised 27 January 2004;
Accepted 5 March 2004

Introduction

Snow, as well as soil frost and thawing, is of importance in mid-latitudes and mountain catchments. Sharratt *et al.* (1997; after Pikul and Aase, 1998) estimated that approximately 50 per cent of the Earth's surface is affected by frozen soil at least during part of the year. Spring snowmelt or frequent melting periods during winter are responsible for a large percentage of annual runoff and also matter flux (Rekolainen, 1989). The temporal variability of the snow cover and spatial heterogeneity of soil freezing – sometimes together with rain-on-snow – causes a complex and dynamic runoff generation (Sui and Koehler, 2001).

Results of erosion studies in northern, central or eastern Europe and North America indicate that the erosion rate during snowmelt events can reach or even exceed the rainfall erosion rate (e.g. Demidov *et al.*, 1995; Edwards *et al.*, 1998; Lundekvam, 2001). Baade (1996) documents the importance of sediment transport during winter for a low mountain environment in SW Germany without further explanation. This study will present another example of the dominance of snowmelt erosion processes in a low mountain region of Germany.

However, most erosion models are developed for rainfall erosion. Snowmelt erosion and related processes of snow accumulation, snowmelt dynamic or soil frost are not described in an appropriate way. Renard *et al.* (1997) exemplify the weakness of the Revised Universal Soil Loss Equation and point out that the estimation of snowmelt erosivity and soil erodibility in cycles of freezing and thawing is problematic. Several deterministic models simulate rill processes but do not take into account the modifications caused by soil frost (Morgan *et al.*, 1998; Laflen *et al.*, 1991). Moreover, in these models the concepts of runoff generation have limitations to describe winter conditions. Therefore, the underlying process to estimate runoff dynamics, runoff erosivity and transport capacity is inadequately modelled.

The main objective of this paper is to characterize the spatial dynamic of soil erosion processes and sediment source areas during snowmelt. The experimental catchment 'Schäfertal' (NE Germany) will be used as an example. A model approach to simulate the runoff generation in the catchment during soil frost conditions, which is passively coupled to an erosion model, is presented.

Material and Methods

The experimental catchment Schäfertal is located in the Harz Mountains, NE Germany, approximately 150 km southwest of Berlin. The outlet of the 1.44 km² catchment is at an elevation of 392 m a.s.l. and the catchment ranges within 83 m. The Luvisols and Cambisols that have developed on the loess sediments on the slopes are intensively used for agriculture (Figure 1). Major crops are winter grain and rape in a rotation of various lengths. Triticale and peas have become more important in the last three years. The Eutric Gleysols and Dystric Gleysols at the valley bottom are utilized for pasture or meadow (see Figure 1). Average annual rainfall is approximately 640 mm; the annual average temperature is 6.8 °C, ranging from -1.8 °C in January to 15.5 °C in July.

The evident seasonality in discharge is mainly caused by variations of evapotranspiration. The discharge varies from less than 10 l s⁻¹ in summer to above 200 l s⁻¹ during the winter period. To a certain extent, a lowered groundwater table that is caused by mining activities in the region since 1970 disturbs the base flow generation. As a consequence, interflow and tile drains dominate the runoff. During flood events an important portion of runoff is generated by fast runoff components such as Horton type, saturated area runoff or preferential flow. On average two or three major snowmelt runoff events occur between January and April.

Since the early 1960s measurements of meteorological and hydrological parameters have been conducted by the University of Applied Science, Magdeburg (Germany) including measurements of soil temperature and snow characteristics (depth, density and water equivalent). A monitoring programme for erosion as well as sediment and nutrient loads was set up in 1998. The regular biweekly sampling scheme for major nutrients and suspended sediments in runoff at the catchment outlet is supplemented by an automatic sampler (ISCO 6700 Series), which collects 24 samples at high water levels at equal time steps. The starting water level for the sampling and the time interval of sampling is seasonally differentiated (2 hours during winter). In addition to water temperature and electric conductivity, the relevant parameters are suspended sediment concentration, total phosphorus, dissolved phosphorus, reactive phosphorus, nitrate, ammonium and dissolved organic carbon. The treatment of the samples and laboratory analysis follow standard procedures. Special attention is paid to measurements of winter runoff generation and erosion since autumn 2000. Erosion is mapped after relevant events.

For the winter period 2001/2002 a measurement scheme was set up to characterize the temporal variability as well as the spatial heterogeneity of soil surface temperature. Results of a preliminary study of temperature in different soil depths show a low thermal conductivity of a typical soil type in the catchment. In consideration of the standard surface cover for meteorological stations (grass), the surface temperature is responding directly to changes in air temperature, which was measured 2 m above ground in time steps of 5 min (Figure 2). Soil surface temperature exceeds the extreme low and high values in the period presented. In contrast, the temperature regime in a depth of 0.1 m is even-tempered and is not following any daily rhythm or other short-term variations. Consequently, fifteen automatic temperature sensors (Tinytalk, Geminidataloggers) were installed in a cross-section through the valley at a depth of 0.05 m for the period from 23 November 2001 until 17 April 2002 with two hours registration time. Different soil types, land use and expositions are represented.

Soil moisture measurements in a depth of *c.* 0.2 m with TDR probes were conducted at the positions of soil temperature measurement (EASY-test FP/mts). Daily readings of the period from 24 November 2001 until 30 April 2003 were used for this study. A longer duration of observation was chosen compared to the temperature values because of probe failures or tillage measures which interrupted the measurement period. The integrated temperature sensors did not indicate situations of soil frost in the relevant depth which might influence the measurement principles.

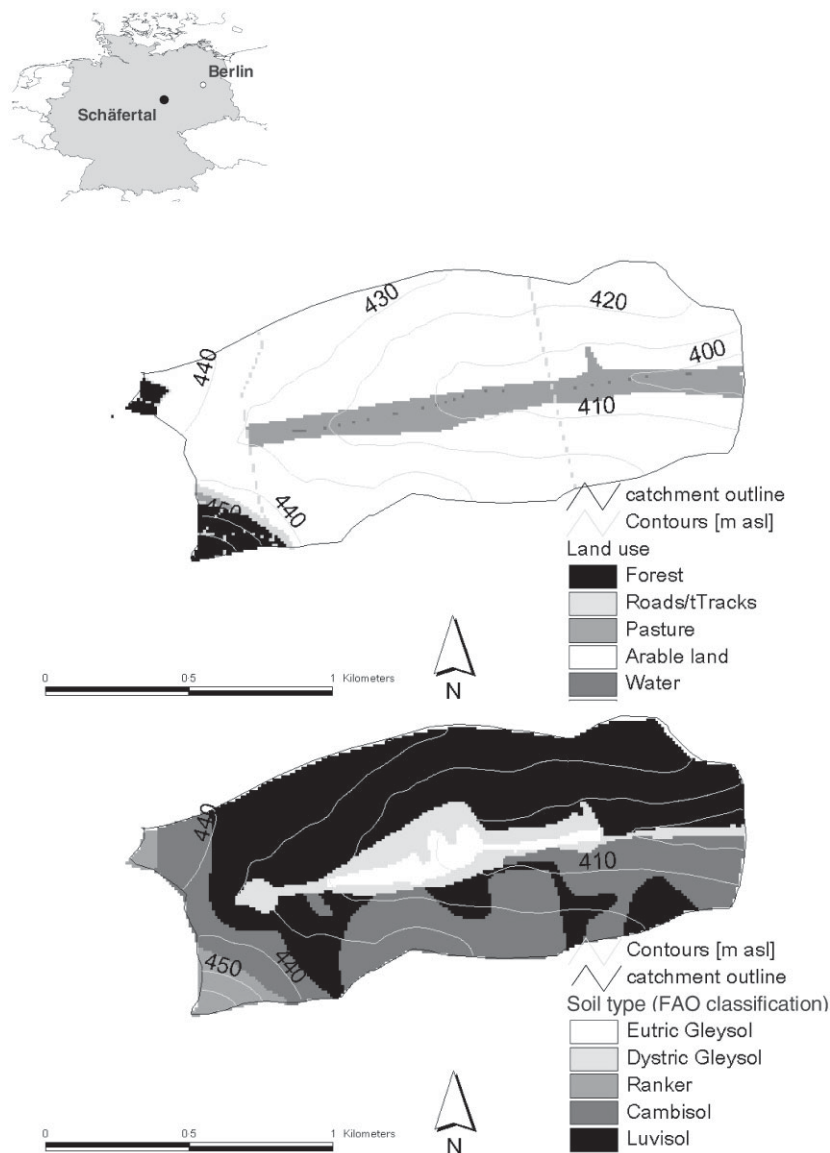


Figure 1. Land use and soil type (FAO classification) of the Schäfertal catchment; inset map shows location of the catchment within Germany.

Results and Discussion

Results and discussion of two events

During the winter periods 2000/2001 and 2001/2002 five periods of snow accumulation and melting occurred; one summer storm event in May 2002 was monitored. Compared to one extensive summer event in June 1999 and data from literature (i.e. Steegen *et al.*, 2000), the suspended sediment concentration (SSC) during the five storms is low and does not exceed 1500 mg l⁻¹. These values are below those which were measured during winter events in a 62 ha catchment in the Kraichgau region (SW Germany) but in the range of concentrations from a 702 ha catchment (Baade, 1996). Difficulties of comparison exist because of differences in slope and portion of arable land. The results from the Schäfertal correspond to measuring data in similar catchments with loess cover (i.e. van Dijk and Kwaad, 1996) or in those with riparian vegetation zones (i.e. McKergow *et al.*, 2003). However, due to runoff volume, the major portion

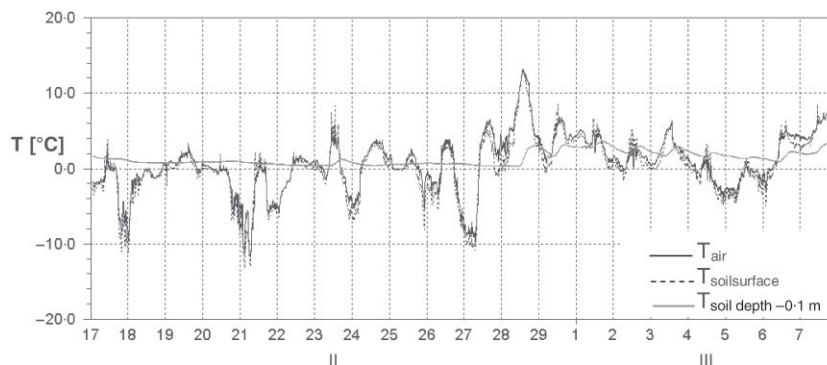


Figure 2. Characterization of air temperature, soil surface temperature and soil temperature at a depth of 0.1 m below the surface in the Schäferfالت catchment for a period in February and March 2001.

Table I. General characteristics of two snowmelt–erosion events in the Schäferfالت catchment

	6 Feb. 2001	20 Jan. 2002
Winter situation	unfrozen soil	frozen soil
Snow water equivalent (mm)	20	50 (17–111)
Discharge max. (l s^{-1})	59	175 (85 for snowmelt)
Runoff volume (m^3)	24 266	76 529, c. 50% from snow
Net erosion (t)	0.36	4.9
SSC max. (mg l^{-1})	35.1	1390
Standard dev. SSC (mg l^{-1})	7.55	231.6
Median SSC (mg l^{-1})	20.1	69.5

of the annual sediment yield of these two years is reaching the catchment outlet during the wintertime. The erosion rate for single winter events which was calculated from total event load varies from 0.0025 t ha^{-1} to 0.034 t ha^{-1} . Probably the pasture area in the central part of the Schäferfالت valley near the channel is acting as a buffer strip for surface runoff and sediment.

The characteristics of the snowmelt erosion events of 6 February 2001 and 20 January 2002 show different possibilities of runoff generation and sediment sources. The net erosion is 0.36 t and 4.9 t, respectively. Table I gives an overview of the general values of the two events that differ in the relevant parameters.

A melting of the snow pack within 24 hours, which had a water equivalent of approximately 20 mm, caused the flood of February 2001 in the Schäferfالت catchment. The high infiltration rate into a predominantly unfrozen soil led to a runoff generation in two stages (Figure 3). The first part of the hydrograph reaches a discharge up to 30 l s^{-1} and represents surface runoff from saturated areas near the channel and fast interflow components. The maximum discharge of 59 l s^{-1} occurred in the second stage of the flood that is generated mainly by interflow, runoff from tile drains and an additional portion of base flow. Suspended sediment concentration shows two peaks of 20.5 mg l^{-1} and 35.0 mg l^{-1} , each of them occurring during the early afternoon. Because of a lack of progressing data it is not clear if this is a diurnal rhythm with partial freezing during the night and decreased erodibility of the sediment source, or if it is due to reduced transport capacity of the flow. The hysteresis curve of this storm is complex and reflects the two sediment concentration peaks as an addition of two clockwise effects (Figure 3). It is evident that either the channel is the sediment source area (Klein, 1984) or the material is recycled sediment from inter-storm periods (Steege *et al.*, 2000). However, field observations during the measurement period reveal morphologic activity at the channel bed and banks and a general trend of incision for the channel over the last two decades.

In contrast, the runoff volume of the event on 20 to 30 January 2002 is three times greater, and is generated from a snow water equivalent of about 50 mm on average (spatial variation from 17 mm to 111 mm depending on wind drift). The net erosion is more than ten times greater and the maximum suspended sediment concentration is 40 times higher than during the snowmelt in February 2001 (see Table I). Due to a long snowmelt, the discharge is constant over a period of five days after a first increase in discharge to approximately 80 l s^{-1} (Figure 4). No diurnal rhythm is observable as a result of air temperature being above freezing point during the night. The maximum discharge of 175 l s^{-1} occurs in a later stage of the event and is triggered by an additional rainfall of about 25 mm. At the beginning

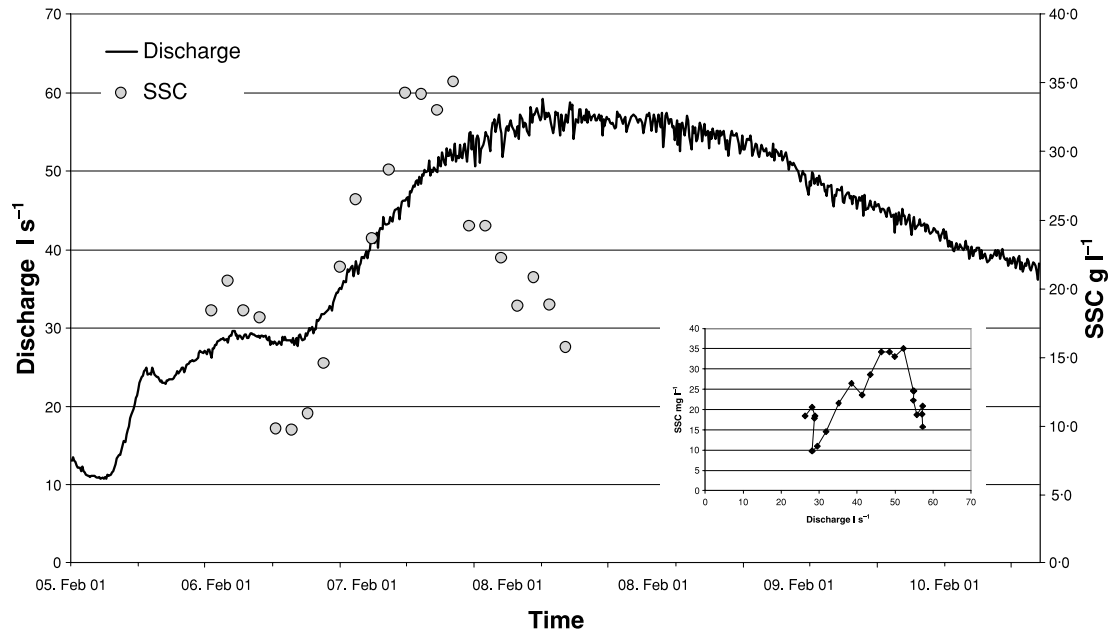


Figure 3. Discharge and suspended sediment concentration (SSC) at the catchment outlet of the Schäferfalter for the event on 6 February 2001; inset graph shows the hysteresis.

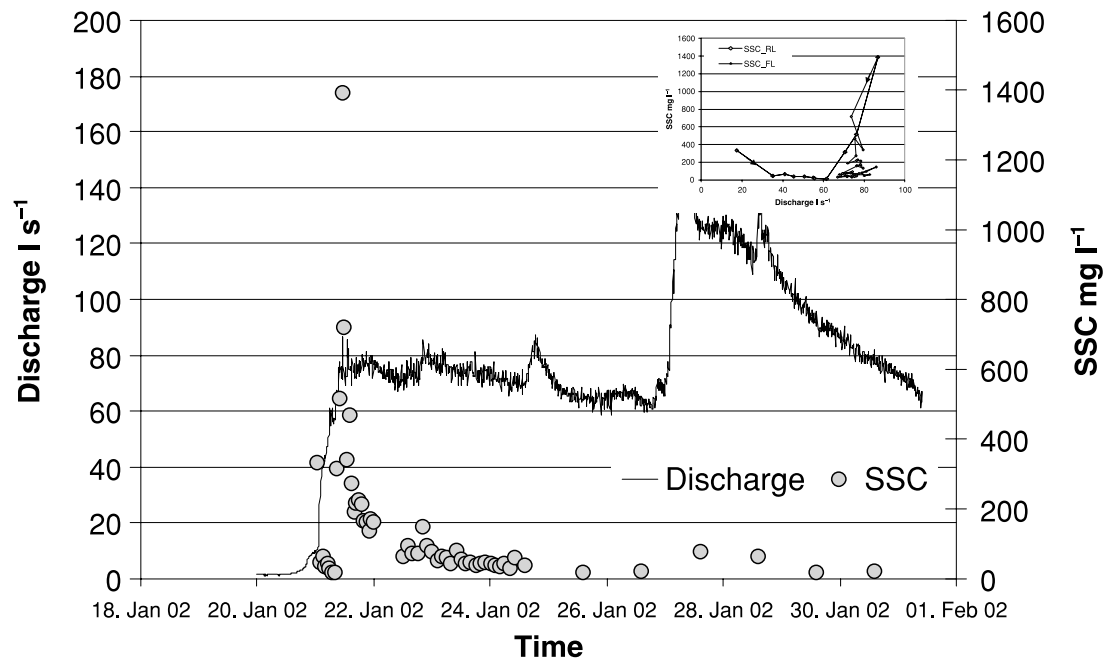


Figure 4. Discharge and suspended sediment concentration (SSC) at the catchment outlet of the Schäferfalter for the event on 20 January 2002; inset graph shows the hysteresis.

of the snowmelt the soil is frozen in the predominant part of the catchment and runoff is generated mainly from melting of water from the snow that is not infiltrating. Due to this fact the runoff is dominated by surface runoff from the slopes. The exceptional ‘falling limb’ of the hydrograph also supports this hypothesis until the onset of the precipitation (see Figure 4). The decrease of the discharge after the peak caused by rainfall is more usual and indicates

Table II. Spearman correlation coefficients of selected parameters of the rising limb (RL) and falling limb (FL) of the event on 20 January 2002

	DOC		SSC		P _{tot}	
	RL	FL	RL	FL	RL	FL
DOC	1.000	1.000				
SSC	-0.014	0.853	1.000	1.000		
P _{tot}	-0.199	0.841	0.744	0.918	1.000	1.000

a thawed or only locally frozen soil. However, the concentration of suspended sediment shows only one peak at the first stage of runoff generation. With 69.5 mg l⁻¹ the median sediment concentration of this event is double the maximum sediment concentration of the snowmelt runoff discussed above. The hysteresis of 50 samples (to the beginning of the influence of the rainfall) is anti-clockwise for the rising limb of the hydrograph that characterizes erosion on the slopes and coincides with field observations (see Figure 4). As a result of constant and high discharge but decreasing sediment concentrations the hysteresis curve falls rapidly to a base value of suspended sediment concentration (SSC). This might be interpreted as a depletion of erodible material on the slopes or a change of the source area to one with less erodible sediment. Although the rainfall on 27 January caused the maximum discharge, no increase in sediment concentration was measured. Additionally, no further evidence of erosion was observed in the catchment. This is in contrast to the extreme gully erosion which is reported for Norway (Øygarden, 2003) and may be due to the fact that the soil was thawed at this time of the event. The variation in correlation coefficients of selected parameters for the rising and falling limb of the hydrograph gives evidence that the characteristic of the sediment has changed (Table II). Contrary to the correlation coefficients for the rising limb, the concentration of dissolved organic carbon (DOC) to SSC and concentration of total phosphorus (P_{tot}) is very high. In addition, the non-parametric Mann–Whitney test to compare two groups shows significant differences between P_{tot} and DOC for the rising and falling limb of the hydrograph ($p < 0.001$). One possible source for the sediment might be the pasture area in the central part of the valley where seepage outflow or exfiltration occurs due to low slopes and reduced lateral flow in the thawed layer of the topsoil (for land use in the catchment see Figure 1). The pasture is characterized by low erodibility and high availability of organic matter and phosphorus. Evidence for this source area is the comparison of the P_{tot} and SSC values of the falling limb to those from the event on 6 February 2001 which was characterized as channel erosion. The results of a Kruskal–Wallis one-way analysis of variance show significantly different values for P_{tot} and SSC of the two events (for P_{tot} $\chi^2 = 29.585$ with 1 df; $P = 0.000$; for SSC $\chi^2 = 11.450$ with 1 df; $P = 0.001$). Aside from this fact, the regression line of the P_{tot} and SSC relationship has a distinctly different slope ($y = 0.0007x + 0.0843$ for the falling limb of 20 January and $y = 0.0038x + 0.124$ for the event of 8 February). These statistical discrepancies are pointing to a variation of the sediment source areas of the two events.

Although the relative portion of winter grain area is comparable, the described situations are characterized by individual processes. The two discussed snowmelt events which lead to sediment output from the Schäfertal catchment differ in prevailing soil frost conditions and as a consequence in net erosion and sediment source area as well as spatial dynamics of source area. The basic cause for the distinction is the modification of runoff generation in situations with frozen soil.

Temporal and spatial dynamic of topsoil temperature

The minimum and maximum air temperature during the period of investigation was -19.6 °C and 16.0 °C, respectively. The minimum soil temperature varied from -5.8 °C to -0.1 °C depending on surface cover and exposition of the sensors in the cross-section. The maximum values ranged between 9.8 °C and 12.5 °C.

Figures 5 and 6 show the performance of the measured air temperature and two soil temperature sensors that are characterized by different exposition. The soil temperature at a depth of 0.05 m reflects the longer meteorological periods of the air temperature (i.e. February 2002 in Figure 5) and the daily rhythm (i.e. April 2002 in Figure 6). Periods of snow cover attenuate the thermal reaction of the soil to a minimum (i.e. January 2002). In principle, this relationship of air and soil temperature is persistent also for data that are aggregated to daily time steps (Figure 7).

Significant differences can be found in the daily temperature values, which are arranged by land use and weaker differences grouped by exposition (probability 0.00 and 0.22 from Kruskal–Wallis test). This is confirmed by a cluster tree analysis (Figure 8). Three major clusters occur: the first for the temperature sensors under pasture, the second and third for the positions under winter grain, which was the dominant crop during winter 2001/2002. The latter two

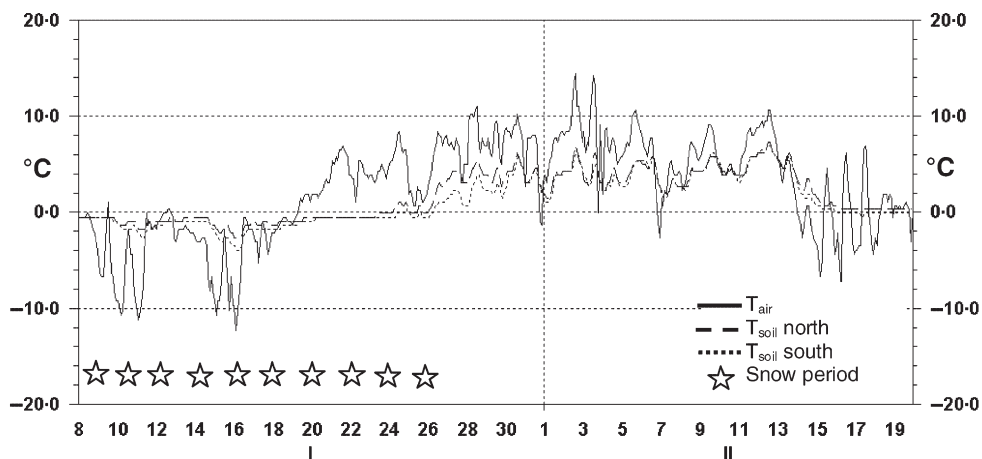


Figure 5. Variation of air temperature and soil temperature at a depth of 0.05 m for north and south exposition with two hour registration time for a cloudy period with precipitation.

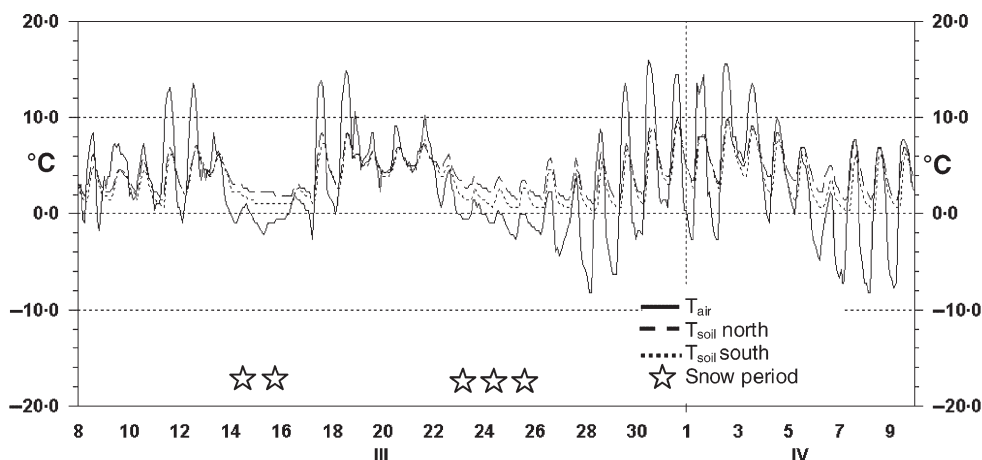


Figure 6. Variation of air temperature and soil temperature at a depth of 0.05 m for north and south exposition with two hour registration time for a cloudless period with daily rhythm.

clusters vary in exposition, but the Euclidean distance is not as high as for pasture. Although sensor S2_7 is located in a pasture area the values are characterized by very high distances to all other measurements. A shallow groundwater table that might have impact on the thermal soil characteristics influences this position. However, land use and exposition are parameters that are not related to one single process in freezing and thawing attitude of a soil. Rather they are summarizing factors for surface structure such as albedo, snow cover dynamic and soil moisture variations, which influence thermal conductivity and heat capacity (Zhao and Gray, 1999; Stadler *et al.*, 1997).

Temporal and spatial dynamic of soil moisture

The daily soil moisture of 3232 measurements varies between 8 and 60 per cent of volume. Both median and mean values are close together at 27.5 per cent which is approximately the effective field capacity of the soils. The cross-section shows clear differences of soil moisture in relation to the position on the slope (Figure 9). In the central part of the valley, near the channel (position f in Figure 9), the soil moisture is highest and often reaches saturation or even over-saturated conditions. Both north and south aspects are characterized by lower soil moisture values than the valley. This typical spatial distribution of soil moisture in the Schäfertal is a result of lateral soil water flow or interflow and a groundwater table in the valley that is temporary near the surface (Buchholz *et al.*, 1998).

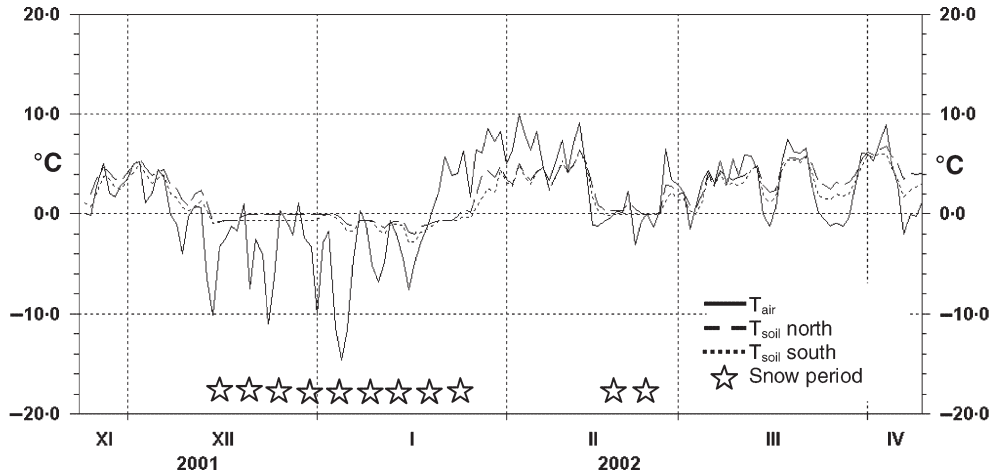


Figure 7. Variation of averaged daily air temperature and averaged daily soil temperature at a depth of 0.05 m for north and south exposition.

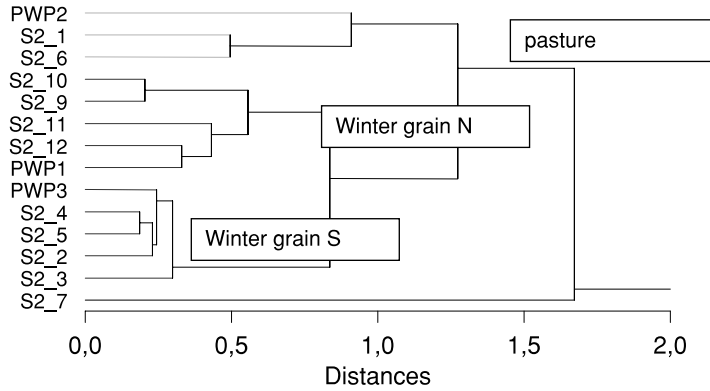


Figure 8. Cluster tree of measured soil temperature variation.

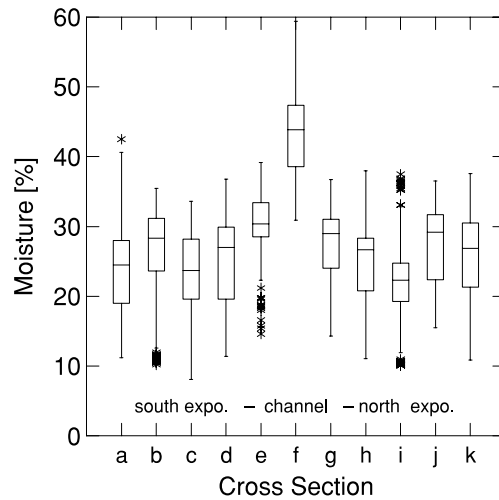


Figure 9. Results of TDR soil moisture measurements of a cross-section in the Schäferfirtal.

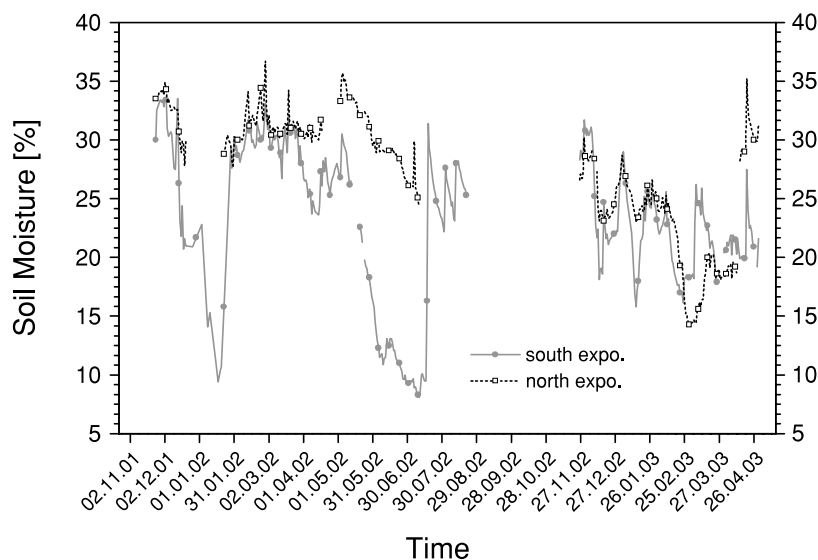


Figure 10. Variability of soil moisture at different expositions.

Although the soil moisture on the slopes is relatively low, significant differences can be identified in the temporal behaviour. Figure 10 shows results of two selected sensors at mid-slope position of the north- and south-facing slope. In general, the TDR sensor of the slope with northern exposition has higher soil moisture values and lower variability. In contrast, the measurements of the south-exposed slope tend to very low values during dry periods in summer and also winter. A Kruskal–Wallis one-way analysis of variance for all sensors on the slopes shows significantly higher soil moisture values for the northern exposition ($P = 0.05$; $\chi^2 = 3.65$ with 1 df).

Famiglietti *et al.* (2001) report numerous contradictions in the interpretation of factors that influence the soil moisture variability, especially topographic parameters. With respect to the uniform slope angle, homogenous soil characteristics and land use in the Schäfertal catchment there is evidence that aspect and depth to groundwater table are the dominant factors to determine the spatial heterogeneity of the soil moisture. These results are in agreement with those presented by Svetlitchnyi *et al.* (2003) for small catchments with homogenous soils in Ukraine, and Gómez-Plaza *et al.* (2001) who modified topographic wetness indices by introducing the factor aspect as ‘an appropriate surrogate of potential insolation’ (p. 224).

The model approach

A passive coupling of the hydrological model WaSim – ETH and the nutrient loading model AGNPS is used to simulate the runoff generation and erosion in the Schäfertal catchment (Lindenschmidt and Rode, 2001). WaSim – ETH is a cell-based distributed model with a modular architecture that provides spatial information about the hydrological aspects of a catchment (Schulla, 1997). This includes evapotranspiration, interception, snow accumulation and melting. It considers different processes of runoff generation, for example Horton-type overland flow or runoff generation from saturated areas. For modelling the water balance of the Schäfertal catchment, Version 2 is used which utilizes a Richard’s equation approach to simulate the soil water budget in daily intervals. During periods of snowmelt a portion of the snowmelt water which can be defined individually is considered to be surface runoff. However, a homogenous snow cover and melting results in spatially undifferentiated surface runoff.

The calculated surface runoff from WaSim replaces the estimation of runoff in AGNPS, which is a SCS-CN approach (for more information about AGNPS see Young *et al.* (1994) and <http://www.sedlab.olemiss.edu/agnps.html>). The improvement in hydrology leads to a better estimation of sediment and nutrient loads at the catchment scale (Lindenschmidt *et al.*, 2004).

On the basis of the field observations described above, a new module is incorporated into the WaSim to enhance the simulation of surface runoff generation during winter periods. Numerous one-dimensional models exist to describe water and heat transfer in frozen or snow-covered soils. They are used as meteorological or climatological prediction models. Only a few models take into account the interaction of snow and soil, i.e. SHAW or SOIL (Isard and Schatzl, 1998; Johnsson and Lundin, 1991; Stadler *et al.*, 1997; Stähli *et al.*, 1999; Zhao *et al.*, 1997). The WEPP model

Table III. General characteristics, correlation coefficients of estimated soil temperature to measured soil temperature and the related polynomial function

Sensor	Land use	Exposition	r	Polynomial function
2_2	Winter grain	S	0.81	$y = 1.59556 + 0.45915x + 0.00638x^2$
2_3	Winter grain	S	0.8	$y = 1.65136 + 0.43058x + 0.00705x^2$
2_4	Winter grain	S	0.78	$y = 1.79153 + 0.43353x + 0.00545x^2$
2_5	Winter grain	S	0.8	$y = 1.44264 + 0.40832x + 0.00935x^2$
PWP3	Winter grain	S	0.79	$y = 1.82279 + 0.418234x + 0.00534x^2$
2_9	Winter grain	N	0.7	$y = 1.67589 + 0.32633x + 0.00467x^2$
2_10	Winter grain	N	0.69	$y = 1.83705 + 0.31845x + 0.00443x^2$
2_11	Winter grain	N	0.78	$y = 1.33826 + 0.37853x + 0.0075x^2$
2_12	Winter grain	N	0.76	$y = 1.61136 + 0.386021x + 0.00828x^2$
PWP1	Winter grain	N	0.76	$y = 1.54354 + 0.37186x + 0.0089x^2$
2_7	Pasture	N	0.79	$y = 3.20209 + 0.30818x + 0.00318x^2$
PWP2	Pasture	N	0.62	$y = 2.2583 + 0.23828x + 0.00226x^2$
2_6	Pasture	E	0.73	$y = 2.0208 + 0.34919x + 0.0029x^2$
2_1	Pasture	E	0.66	$y = 2.5491 + 0.30957x - 0.00084x^2$

Table IV. Generalized coefficients of the polynomial function to estimated soil temperature

	$C_{land\ use}$	$C_{exposition}$	$C_{undefined}$
Winter grain	1.631		
Pasture	2.508		
E		0.3293	
N		0.3325	
S		0.4299	
All sensors			0.0055

utilizes an energy budget approach to estimate snow depth and soil frost occurrence (http://www.ars.usda.gov/research/publications/publications.htm?SEQ_NO_115=152825). In general, the data demand of these models is high and the possibility of calibration or verification in a catchment is low. Simpler approaches to estimate the occurrence of soil frost exist for the modification of the CREAMS model for Finnish conditions (Rekolainen and Posch, 1993) or the Suckow algorithm, which is used in ARCEGMO (<http://www.arcegmo.de/public/index.htm>). In contrast, one basic requirement for the new module for WaSim is a minimum input of data and a spatial differentiation in the results.

The measured data of air temperature and soil temperature from the Schäferfalter catchment were subject to a curve-fitting procedure to develop an easy tool to estimate the temperature of the topsoil. The data from one sensor (S2_8) were excluded because the sensor was exposed by burrowing animals during the measurement period. Also, the periods with snow cover were excluded. A second-order polynomial achieves the best agreement of estimated soil temperature on the basis of air temperature. Correlation coefficients vary from 0.62 to 0.81 with an average of 0.75. Table III shows the agreement and the polynomial function for the sensors. The constants are modified based on the knowledge of significant differences of measured soil temperature depending on land use and exposition. The outcome of this is an estimation of the topsoil temperature T_{soil} :

$$T_{soil} = C_{land\ use} + C_{exposition} * T_{air} + C_{undefined} * T_{air}^2$$

with T_{air} as measured air temperature and $C_{land\ use}$, $C_{exposition}$ as constants for land use and exposition, respectively (Table IV). $C_{undefined}$ is constant for all positions but might be differentiated with further results to improve the fitting. Although the differentiation of soil moisture is to a high degree explained by aspect, it might be one of the arguable variables for the calculation. More data from a longer time period and other land uses as well as other catchments are needed to ensure this approach. However, for the Schäferfalter this simple soil temperature model based on measured air temperature values works reliably.

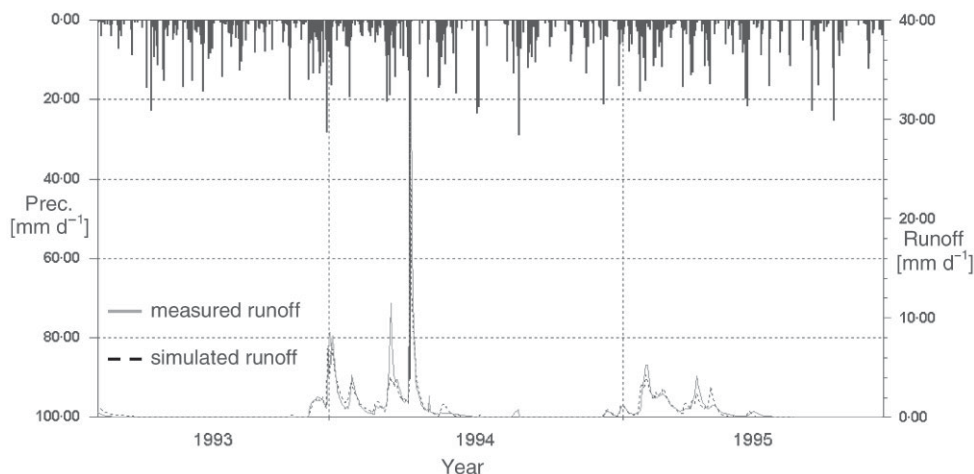


Figure 11. Daily precipitation, observed and simulated runoff with WaSim for the Schäfertal catchment.

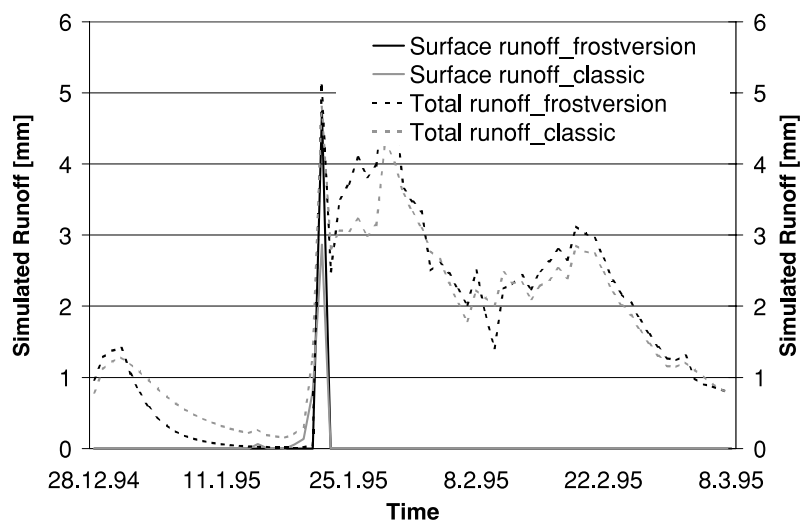


Figure 12. Comparison of simulated runoff with the original version (classic) and the modified version (frostversion) of WaSim for a snowmelt event in January 1995.

The algorithm was implemented into the architecture of WaSim as a separate module. For days with a calculated snow water equivalent of more than 5 mm the estimated soil temperature of the previous day is used. The calculation is executed for each time step and for each cell. Although the impact of frozen soil on infiltration is variable, a number of studies report a strong decrease of hydraulic conductivity (i.e. Seyfried and Murdock, 1997; Hayashi *et al.*, 2003). Consequently, the saturated hydraulic conductivity of the soil is assumed to be zero for the individual grid cell when the soil is frozen. This simplified assumption was drawn with respect to the low data demand and lack of accurate verification possibilities at the catchment scale.

The first test of the modified hydrological model WaSim is conducted for the winter period 1994/1995 for which the general agreement of observed and simulated runoff is reliable ($r^2_{1994} = 0.88$; $r^2_{1995} = 0.84$) (Figure 11). This guarantees an independent control for the model. In January 1995 a soil frost situation and surface runoff generation from snowmelt occurred. In general, the total simulated runoff from the original version and the modified model differ slightly for the period before the snowmelt, with lower runoff caused by reduced infiltration into the frozen soil (Figure 12). The peak runoff for the dominant day of snowmelt (25 January 1995) is nearly equal for both versions but the initiation of snowmelt runoff in the original version is one day before the model with soil frost modelling. As a consequence of modified soil moisture conditions, the simulated total runoff for the frost modification is higher after

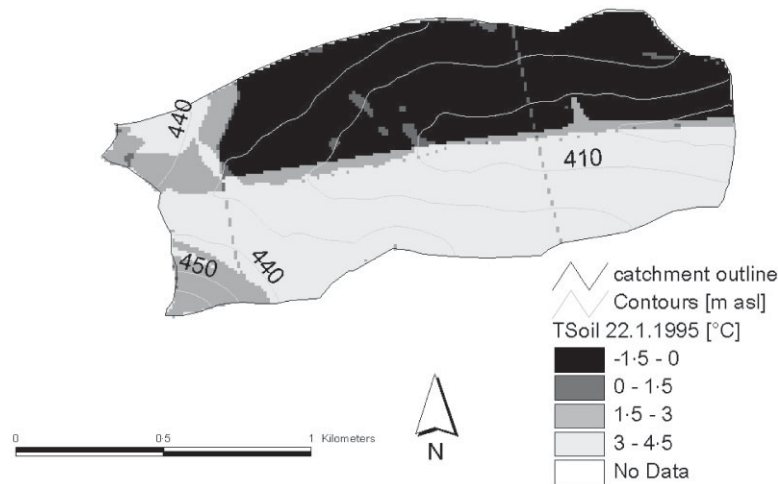


Figure 13. Estimated spatial distribution of soil temperature for 22 January 1995 with the modified version of WaSim.

the snowmelt. The model results converge towards the end of the simulation period. There are distinct differences in simulated surface runoff generation, although the total runoff volume during the peak of the snowmelt is similar (see Figure 12). The portion of surface runoff for the original version is defined by a constant parameter and does not reach 3 mm in the example. In contrast, the version with soil frost and the related soil conductivity modification generates 95 per cent of the total runoff of the relevant day as surface runoff.

In addition to the temporal differences, the spatial aspects of runoff generation are of importance for erosion and sediment transport. The estimated topsoil temperature for 22 January 1995, the day of peak runoff during the snowmelt, divides the Schäfertal catchment in two parts (Figure 13). The north-facing slopes reach a temperature above zero. In contrast, most of the area on the slope with southern exposition is frozen. Although this seems to be abnormal because the insolation on the south-facing slope is higher, it can be explained by differences in soil water balance. The daily measurements of soil moisture the Schäfertal show a distinct difference in soil moisture of the two slopes. In general, as a result of higher evapotranspiration, the south-facing slope is much dryer. Thus, the heat capacity of the soil is lower and freezing takes place earlier than on slopes with moister northern exposition. The simple soil temperature model obviously reflects the dominant processes that are important for the spatial heterogeneity of soil frost. The occurrence of soil frost obverts the spatial heterogeneity of runoff generation which had to be expected from the soil moisture distribution. Field observations confirm this fact. Despite separated process knowledge (snow accumulation, snowmelt, freezing–thawing of soil, infiltration into frozen soil) no reference was found to approve this combination at a catchment scale.

The spatial heterogeneity in soil frost appearance is the basis for a spatially differentiated consideration of surface runoff generation. On the basis of the modified soil hydraulic conductivity WaSim simulates surface runoff generation on the south-facing slope where the soil is frozen (Figure 14). Runoff occurs after the pore volume is filled up. Antecedent soil moisture and soil characteristics provoke a patchwork of runoff. In addition, saturated area runoff is generated in non-frozen areas.

Although the estimation of erosion in AGNPS is not suitable for winter conditions, the result of the passive coupling from WaSim to AGNPS leads to a spatially plausible calculation of sediment yield (Figure 15). The sediment yield is high in the areas where the runoff is concentrated in shallow depressions and reaches the channel only at a small number of locations. Maximum sediment yield occurs in the channel a few hundred metres before the catchment outlet and measurement devices. The entrance points for runoff and sediment from the slope to the stream can be verified by field observations. The spatial distribution of runoff generation and erosion as well as the dimension of sediment yield is plausible and the results of the simulation can be approved by field observations from other events. In general, the modified model is robust and reliable. A first version of a snowmelt erosion model for rill erosion is tested and coupled to WaSim (Ollesch *et al.*, 2003). Due to the simplicity of the soil temperature estimation which is restricted to the topsoil, the transferability of the model and the results is limited. However, unreliable results in model application are often caused by inadequate calculation of runoff generation. This is especially true for winter conditions for which Pannkuk *et al.* (1998) and Ranaivoson *et al.* (2001), for example, demonstrated unsatisfactory results from the WEPP model.

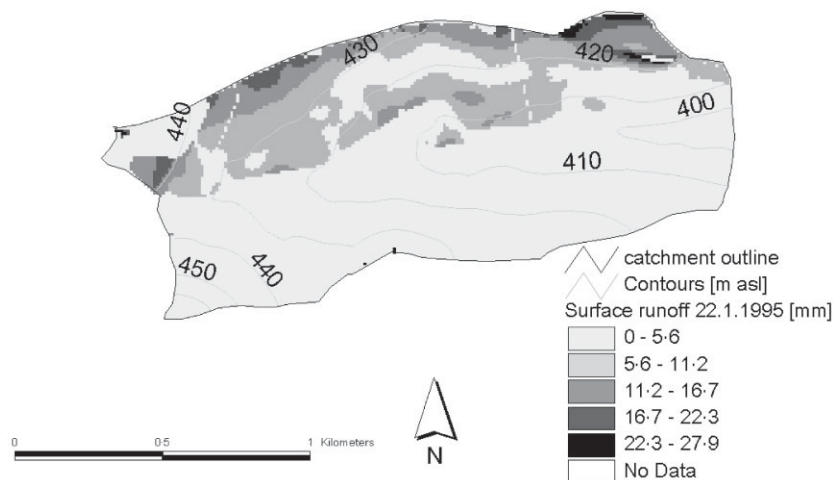


Figure 14. Estimated spatial distribution of surface runoff for 22 January 1995 with the modified version of WaSim.

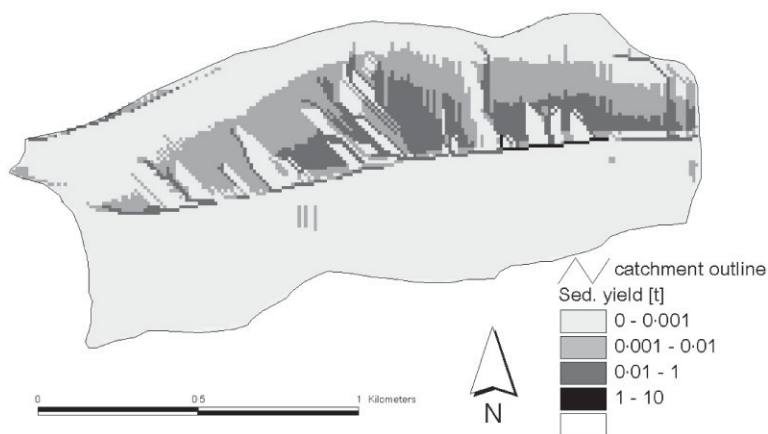


Figure 15. Estimated spatial distribution of sediment yield for 22 January 1995 with AGNPS after coupling with WaSim.

Conclusions

The occurrence of snowmelt and frozen soil as well as related erosion events has a spatial dimension. The data from the Schäferfalter catchment show that surface runoff generation in winter can cause higher erosion rates than summer events. The described snowmelt event in combination with soil frost is characterized by a suspended sediment concentration that is 40 times higher than for a runoff event without frozen soil.

In consequence, a model has to reflect the heterogeneity of important parameters for winter situations in an entire catchment. This is of particular importance for soil freezing and thawing that affect the generation of surface runoff and also the soil erodibility. The modified continuous hydrological model WaSim provides a fruitful endeavour to model this phenomenon for the following reasons:

- (i) insertion of a simple empirical but effective tool to estimate soil temperature and soil frost situations depending on land use and exposition;
- (ii) modified water infiltration into the soil at frozen conditions;
- (iii) plausible spatial surface runoff generation at winter conditions including the generation of Horton-type runoff and saturated area runoff.

The modification presented of the model WaSim which is passively coupled to AGNPS works consistently. A further modification of the estimation of soil erosion based on processes is required and is in preparation.

Acknowledgement

This work is financed by the German Federal Ministry of Education and Research (BMBF) and is part of the joint German-Russian Project 'Volga-Rhine'. Contract number 02WT0099. We thank Dr A. Vacca, University of Cagliari, Italy, for critical comments. The authors also thank G. Wenk, University of Applied Science Magdeburg, for discussion and the fruitful co-operation in the Schäfertal.

References

- Baade J. 1996. Spatial and temporal variability of discharge and sediment yield in small loess-covered catchments. *Géomorphologie: Relief, Processes, Environment* **3**: 65–74.
- Buchholz K, John H, Senst M, Wenk G. 1998. *Differenzierte Untersuchung des Abflußkomponentenregimes hydrologischer Untersuchungsgebiete unter den Bedingungen von Bergbaufolgebemaßnahmen und Bewertung geoökologischer Auswirkungen als Beitrag zum Hochwasserschutz und zur Sicherung der Wassergüte der Selke*. Final report Volume I/II, IWM Institut für Wasserwirtschaft GmbH of the FH: Magdeburg.
- Demidov VV, Ostroumov VY, Nikitishena IA, Lichko VI. 1995. Seasonal freezing and soil erosion during snowmelt. *Eurasian Soil Science* **28**: 78–87.
- Edwards L, Richter G, Bernsdorf B, Schmidt R-G, Burney J. 1998. Measurement of rill erosion by snowmelt on potato fields under rotation in Prince Edward Island (Canada). *Canadian Journal of Soil Science* **78**: 449–458.
- Famiglietti JS, Rudnicki JW, Rodell M. 2001. Variability in surface moisture content along a hillslope transect: Rallessnake Hill, Texas. *Journal of Hydrology* **210**: 259–281.
- Gómez-Plaza A, Martínez-Mena M, Albaladejo J, Castillo VM. 2001. Factors regulating spatial distribution of soil water content in small semiarid catchments. *Journal of Hydrology* **253**: 211–226.
- Hayashi M, van der Kamp G, Schmidt R. 2003. Focused infiltration of snowmelt water in partially frozen soil under small depressions. *Journal of Hydrology* **270**: 214–229.
- Isard SA, Schaetzl RJ. 1998. Effects of winter weather conditions on soil freezing in Southern Michigan. *Physical Geography* **19**: 71–94.
- Johnsson H, Lundin L-C. 1991. Surface runoff and soil water percolation as affected by snow and soil frost. *Journal of Hydrology* **122**: 141–159.
- Klein M. 1984. Anti clockwise hysteresis in suspended sediment concentrations during individual storms: Holbeck catchment; Yorkshire, England. *Catena* **11**: 251–257.
- Lafen JM, Lane LJ, Foster GR. 1991. WEPP: A new generation of erosion prediction technology. *Journal of Soil and Water Conservation* **46**: 34–38.
- Lindenschmidt K-E, Rode M. 2001. Linking hydrology to erosion modelling in a river basin decision support and management system. In *Integrated Water Resources Management*, Symposium Proceedings, Davis, California, April 2000. IAHS Publication **272**: 243–248.
- Lindenschmidt K-E, Ollesch G, Rode M. 2004. Physically-based hydrological modelling for non-point dissolved phosphorus transport in small and medium-sized river basins. *Journal of Hydrological Science* **49**: 495–510.
- Lundekvam H. 2001. ERONOR/USLENO, new empirical erosion models for Norwegian conditions. *International Symposium on Snowmelt Erosion and Related Problems*, 28–30 March 2001, Oslo, Norway.
- McKergow LA, Weaver DM, Prosser IA, Grayson RB, Reed AEG. 2003. Before and after riparian management: sediment and nutrient export from a small agricultural catchment, western Australia. *Journal of Hydrology* **270**: 253–272.
- Morgan RPC, Quinton JN, Smith RE, Govers G, Poesen JWA, Auerswald K, Chisci G, Torri D, Styczen ME, Folly AJV. 1998. *The European Soil Erosion Model (EUROSEM): Documentation and User Guide. Version 3.6*. Silsoe College, Cranfield University.
- Ollesch G, Sukhanovski Y, Demidov V. 2003. A new approach to model rill erosion during snowmelt. *Book of Abstract and Field Guide COST 623 Final Meeting and Conference*, 5–8 July 2003, Budapest, Hungary.
- Øygarden L. 2003. Rill and gully development during extreme winter runoff event in Norway. *Catena* **50**: 217–242.
- Pannkuk CD, McCool DK, Mutch PW. 1998. Effects of canopy cover on soil loss. *Annual International Meeting for the American Society of Agricultural Engineers*, Orlando, FL. Paper No. 982062.
- Pikul JL, Aase JK. 1998. Fall contour ripping increases water infiltration into frozen soil. *Soil Science Society of America Journal* **62**: 1017–1024.
- Ranaivoson AZH, Gupta SC, Moncrief JF. 2001. WEPP simulated tillage effects on runoff and sediment losses in a corn-soybean rotation. In *Sustaining the Global Farm*, Stott DE, Mohtar RH, Steinhardt GC (eds). Selected papers from the 10th International Soil Conservation Organization Meeting, 24–29 May 1999, Purdue University and the USDA-ARS National Soil Erosion Laboratory.
- Rekolainen S. 1989. Effect of snow and soil frost melting on the concentrations of suspended solids and phosphorus in two rural watersheds in Western Finland. *Aquatic Science* **51**(3): 211–223.
- Rekolainen S, Posch M. 1993. Adapting the CREAMS model for Finnish conditions. *Nordic Hydrology* **24**: 309–322.
- Renard KG, Foster GR, Weesies GA, McCool DK, Yolder DC. 1997. *Predicting soil erosion by water: A guide to conservation planning with the revised universal soil loss equation (RUSLE)*. Agriculture Handbook No. 703, US Department of Agriculture: 404.

- Schulla J. 1997. *Hydrologische Modellierung von Fliessgebieten zur Abschätzung der Folgen von Klimaänderungen*. Dissertation ETH 12018, Verlag Geographisches Institut ETH Zurich.
- Seyfried MS, Murdock MD. 1997. Use of air permeability to estimate infiltrability of frozen soil. *Journal of Hydrology* **202**: 95–107.
- Stadler D, Flühler H, Jansson P-E. 1997. Modelling vertical and lateral water flow in frozen and sloped forest soil plots. *Cold Regions Science and Technology* **26**: 181–194.
- Stähli M, Jansson P-E, Lundin L-C. 1999. Soil moisture redistribution and infiltration in frozen sandy soils. *Water Resources Research* **35**: 95–103.
- Steege A, Govers G, Nachtergaele J, Takken I, Beuselinck L, Poesen J. 2000. Sediment export by water from an agricultural catchment in the loam belt of central Belgium. *Geomorphology* **33**: 25–36.
- Sui J, Koehler G. 2001. Rain-on-snow induced flood events in Southern Germany. *Journal of Hydrology* **252**: 205–220.
- Svetlitchnyi AA, Plotnitskiy SV, Stepovaya OY. 2003. Spatial distribution of soil moisture content within catchments and its modelling on the basis of topographic data. *Journal of Hydrology* **277**: 50–60.
- Van Dijk PM, Kwaad FJPM. 1996. Runoff Generation and soil erosion in small agricultural catchments with loess-derived soils. *Hydrological Processes* **10**: 1049–1059.
- Young RA, Onstad CA, Bosch DD, Anderson WP. 1994. *Agricultural Non-Point Source Pollution Model, Version 4.03 AGNPS User's Guide*.
- Zhao L, Gray DM. 1999. Estimating snowmelt infiltration into frozen soils. *Hydrological Processes* **13**: 1827–1842.
- Zhao L, Gray DM, Male DH. 1997. Numerical analysis of simultaneous heat and mass transfer during infiltration into frozen ground. *Journal of Hydrology* **200**: 345–363.